Middle East Journal of Science

https://dergipark.org.tr/mejs **MEJS**

e-ISSN:2618-6136

Research Article

OPTICAL, MORPHOLOGICAL, STRUCTURAL, AND PHOTOCATALYTICAL PROPERTIES OF PLASMONIC AU NPS PRODUCED BY PULSED LASER DEPOSITION

İlhan CANDAN**[1] Serap YİĞİT GEZGİN[2] Hadice BUDAK GÜMGÜM[3]
Hamdi ŞÜKÜR KILIÇ[2,4,5]

[1] Dicle University, Faculty of Science, Department of Physics, Diyarbakir, Türkiye
[2] Selcuk University, Faculty of Science, Department of Physics, Konya, Türkiye
[3] Dicle University, Faculty of Science, Department of Physics, Diyarbakir, Türkiye
[4]University of Selçuk, High Technology Research and Development Center (ILTEK), Konya, Türkiye
[5]University of Selçuk, Directorate of Laser Induced Proton Therapy App. and Research Center, Konya, Türkiye
* Corresponding author; ilhan.candan@dicle.edu.tr

Abstract: *Plasmonic Au NPs exhibit exceptional optical, morphological, and structural properties, making them promising materials for applications in photocatalysis, sensing, and energy conversion. This study explores the synthesis and characterization of plasmonic gold NPs produced by pulsed laser deposition, a versatile physical vapor deposition technique. Pulsed Laser Deposition enables precise control over NP formation through tunable parameters such as laser fluence, ambient gas environment, and deposition duration. The resulting NPs were systematically analyzed to evaluate their optical properties, including localized surface plasmon resonance, as well as their morphological and structural attributes. The localized surface plasmon resonance behavior of the synthesized Au NPs was found to be highly dependent on particle size, shape, and distribution, as revealed by UV-Vis spectroscopy and electron microscopy. Structural analysis via X-ray diffraction confirmed the crystalline nature of the NPs, with lattice parameters correlating to their stability and catalytic efficiency. Photocatalytic activity tests demonstrated that the gold NPs could effectively degrade organic pollutants under visible light, leveraging their strong LSPR-induced hot electron generation and charge transfer properties. In this study, gold NP thin film was produced on microscopic glass by Pulsed Laser Deposition system. Gold NPs thin film photocatalyst efficiency 95.00% and reaction rate constant 0.39 min^{-1} were calculated. At the end of 210 min, MB dye was degraded and turned into high transparency due to localized surface plasmon resonance property of gold NP. The findings may provide valuable insights into the design and application of plasmonic Au NPs in photocatalysis and other advanced technologies.*

Keywords*: Au NP, thin film, PLD, LSPR; photocatalyst*

Received: November 20, 2024 *Accepted: December 24, 2024*

1. Introduction

Plasmonic Gold nanoparticles (Au NPs) have garnered significant attention in recent years due to their unique optical, morphological, and structural properties, which make them highly versatile for applications in fields such as photonics, sensing, biomedicine, and environmental remediation [1-5]. One of their most compelling features is the localized surface plasmon resonance (LSPR) phenomenon, wherein the conduction electrons on NP surface oscillate coherently in response to incident light [6-8]. This results in strong light absorption and scattering in the visible and near-infrared regions, which can be finely tuned by manipulating the size, shape, and surrounding medium of the NPs. In addition to their

remarkable optical properties, AuNPs exhibit high stability, biocompatibility, and catalytic activity, making them attractive candidates for photocatalytic applications such as pollutant degradation and solar energy harvesting [9-11].

The synthesis of Au NPs is a critical determinant of their properties and subsequent performance. Among the various methods available, PLD has emerged as a powerful technique for producing plasmonic NPs with tailored characteristics [12-14]. PLD involves ablating a gold target using high-energy laser pulses in a controlled environment, leading to the formation of NPs with unique properties that are challenging to achieve through conventional chemical synthesis. This physical deposition method offers several advantages, including the ability to operate in solvent-free environments, precise control over deposition parameters, and the capacity to produce NPs with uniform size distributions and minimal chemical contamination. Furthermore, using PLD allows for the customization of NP properties by adjusting key parameters such as laser fluence, ambient gas type and pressure, and substrate material [15].

The optical, morphological, and structural characteristics of Au NPs synthesized by PLD have been extensively studied to understand their correlation with functionality. For example, the size and shape of NPs, as well as their surface roughness and spatial distribution, significantly influence their LSPR behavior and photocatalytic activity [16]. Morphological tuning can enhance light absorption efficiency and increase the density of reactive sites, thus improving photocatalytic performance [17, 18]. Structural properties, such as crystallinity and lattice defects, also play a critical role in determining NPs' stability and catalytic activity.

In addition to their intrinsic properties, plasmonic Au NPs are increasingly being explored for photocatalysis, where they act as light absorbers, charge carriers, or electron mediators to drive chemical reactions under light irradiation [19, 20]. The strong LSPR effect enhances local electromagnetic fields and facilitates the generation of hot electrons, which can be transferred to adsorbed molecules to initiate catalytic reactions. Such properties make Au NPs highly effective for environmental applications, including the degradation of organic pollutants and the reduction of toxic compounds. However, optimizing their photocatalytic performance requires a detailed understanding of the interplay between their structural, morphological, and optical attributes.

This study investigates the optical, morphological, structural, and photocatalytic properties of Au NPs synthesized using PLD. By systematically analyzing these attributes, we aim to establish a comprehensive understanding of how the synthesis conditions influence NP performance. The findings provide valuable insights into the design and application of plasmonic Au NPs in photocatalysis and other advanced technologies.

2. Materials and Methods

2.1. Experimental

The synthesis of gold Au NPs was performed using PLD system. The process employed a pulsed Nd:YAG laser operating at a fundamental wavelength of 1064 nm, with pulse durations of 5 ns and a repetition rate of 10 Hz. This laser system is capable of generating second, third, and fourth harmonics at wavelengths of 532 nm, 355 nm, and 266 nm, respectively. For this study, the fundamental wavelength of 1064 nm was selected. A neutral density filter was utilized to control the laser pulse energy before focusing the beam using a lens, as depicted in Fig. 1a.

Glass microscope slides were used as substrates for depositing Au NPs. These substrates were meticulously cleaned using a multi-step procedure involving soap solution, followed by sequential rinsing with isopropyl alcohol and acetone, each for 15 minutes. The cleaning process was further enhanced by ultrasonic treatment, and the substrates were dried using a nitrogen gas stream.

Commercially available high-purity Au sputtering targets (99.99%, Plasmaterials, USA) were used. To ensure uniform ablation and prevent damage to the targets, both the targets and substrates were mounted on independently rotating holders, allowing each laser pulse to strike a fresh area of the target. This setup produced homogeneous NP coatings, as shown in Fig. 1a. The target-to-substrate distance was fixed at 5 cm, and laser deposition was carried out at room temperature.

For the experiments, the laser energy was changed from 15, 20, 25, and 35 mJ per pulse for Au(1), Au(2), Au(3), and Au(4), respectively. The laser beam was focused onto the targets using a lens with a focal length of 50 cm, and the beam was oriented at a 45° angle to the target surface. The energy density for 35 mJ pulse increases significantly to about 2.43 MJ/m² (or 242.81 J/cm²) due to a smaller focused spot size at the focal point. The experiments were conducted in a high vacuum environment, maintaining a pressure of approximately $5x10^{-7}$ mbar. Different NP sizes were achieved by varying the laser power at fixed pulse number applied to the targets. Au(1), Au(2), Au(3), and Au(4) thin films corresponded to 6,000 laser pulses as the laser power varied as 15, 20, 25, and 35 mJ per pulse, respectively. The optical properties of Au NPs were obtained by UV-Vis-NIR spectroscopy (V-670 Jasco, Japan). The Au(4) sample was further investigated by obtaining the following analysis. The morphological and structural properties of Au(4) NPs were investigated by Atomic Force Microscopy (AFM) (NT-MDT/Ntegra Solaris, Ireland), Scanning Electron Microscopy (SEM) (ZEISS EVO LS10, Germany), and X-Ray Diffraction (XRD) (BRUKER D8 ADVANCE, Germany), respectively.

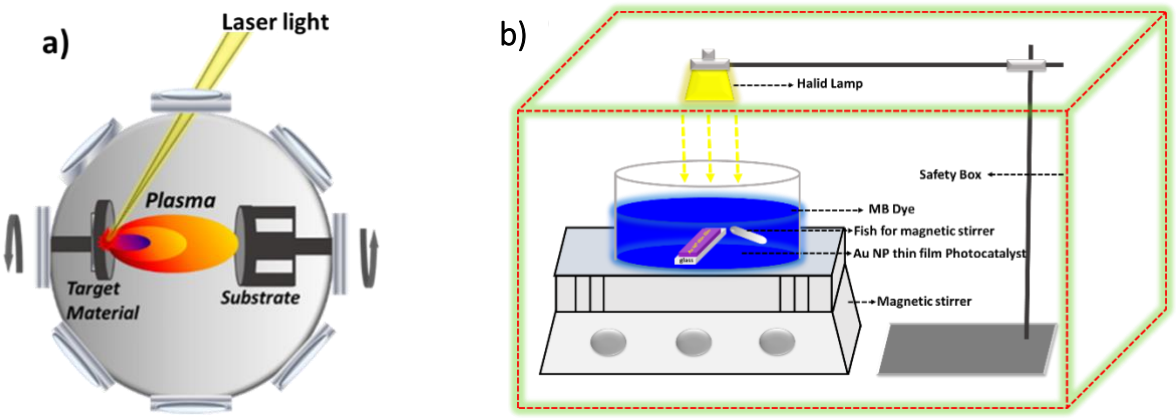

Figure 1. a) The schematic images of PLD and **b)** the photocatalyst systems

100 ml of MB dye was poured into the container in Figure 1b. The fish stirrer and Au NP thin film were placed in the solution and 1000 microliters of base solution (pH=10) were added. The magnetic stirrer was turned on and first kept in the dark for 30 minutes, then liquid was taken under visible light (250 W metal halide lamp (GE ARC250)) every 30 minutes for up to 210 minutes.

3. Results and Discussion

3.1. Structural Properties

Figure 2 shows XRD spectrum of produced plasmonic Au NPs. Peak at ~20°; this peak likely corresponds to the amorphous nature of soda-lime glass, primarily from SiO_2 (silicon dioxide). Peak at ~30°; this peak may arise due to $CaCO_3$ (calcium carbonate) or other crystalline impurities like Na_2SiO_3 present in soda-lime glass. Crystalline calcium-containing compounds can produce reflections in this region, especially under deposition or heat treatment processes. Peak at ~40°; this peak corresponds to the (111) diffraction plane of gold (Au) in a face-centered cubic (FCC) structure. For gold, the (111) peak typically appears at $2\theta \approx 38.2°$ for Cu Kα radiation. Nanoparticle size effects, strain, or substrate interactions can cause slight shifts or broadening of the peak. The expected XRD peaks at 2θ values of 38.18°, 44.38°, 64.57°, and 77.56° correspond to (111), (200), (220), and (311) planes of Au NPs, although the last three peaks are not visible in the XRD spectrum. These diffraction peaks align with the face-centered cubic phase of gold, as referenced in JCPDS file 65-2870 [21, 22]. In the literature, similar research on XRD pattern has been reported for biosynthesized Au NPs, indicating a face-centered cubic structure [23].

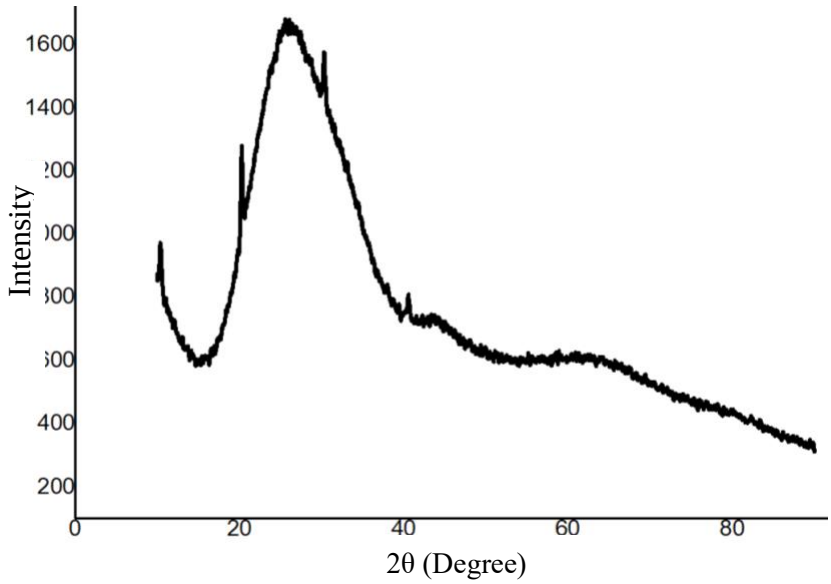

Figure 2. XRD spectrum of plasmonic Au(4) NPs.

3.2. Optical Properties

The optical properties of the produced Au NPs were investigated by UV-Vis-NIR spectroscopy as shown in Figure 3. LSPR peaks of Au NPs were measure to be 925, 685, 655, and 600 nm for Au(1), Au(2), Au(3), and Au(4), respectively. The peaks appeared at the regions of visible as well as infrared spectra. As the laser power increased, LSPR peaks shifted to longer wavelengths (redshift). The reason is at low laser power, small sized Au NPs were produced, and thus, the wavelength of LSPR peak is relatively shorter. Whereas at higher laser power, the larger Au NPs were produced and therefore, the peaks are at longer wavelength.

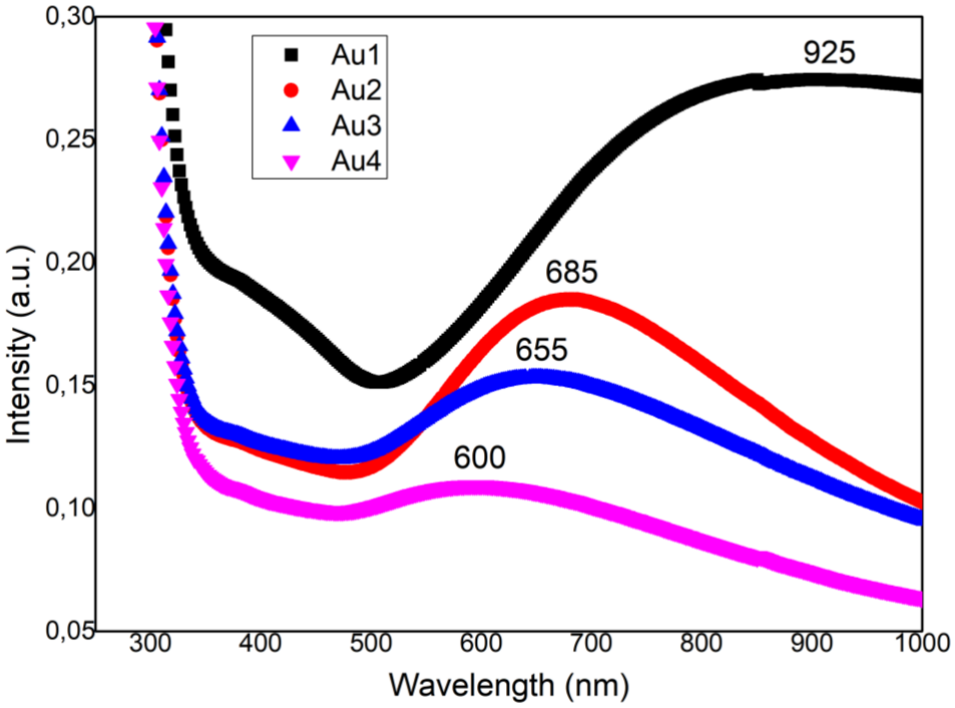

Figure 3. LSPR peak of produced plasmonic Au NPs. The peaks ranges from 600 to 925 nm as the laser power varied.

3.3. Morphological Properties

Figure 4 and 5 illustrates the 2D and 3D AFM images of produced Au NPs. As can be deduced from the pictures, NP sizes are around 100 nm. Roughness values are as follows: S_y= 154.9 nm, S_z = 76.0 nm, Average = 26.5 nm, S_a = 4.9 nm, S_q = 10.1 nm, S_{sk} = 4.7 nm, S_{ka} = 33.9 nm.

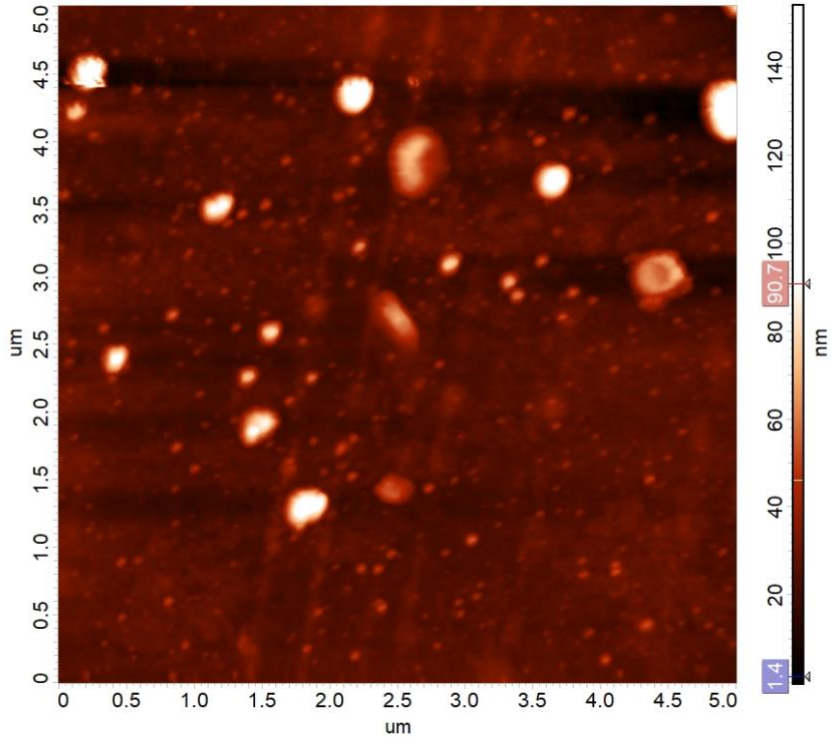

Figure 4. 2D-AFM image of plasmonic Au(4) NPs.

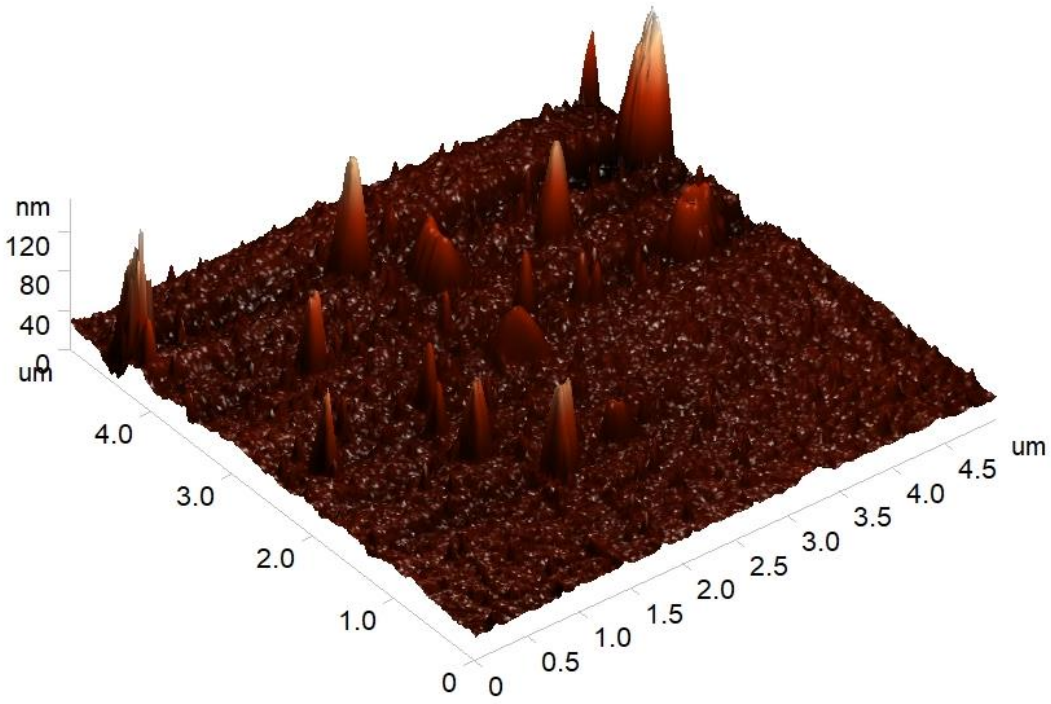

Figure 5. 3D-AFM image of plasmonic Au(4) NPs.

Figure 6 shows SEM image of produced Au NPs and inset of the left demonstrate Au NP thin film that is fabricated on a glass in the lab. The images provide that the produced Au NPs are spherical in shape and the particles are almost uniformly distributed on the glass.

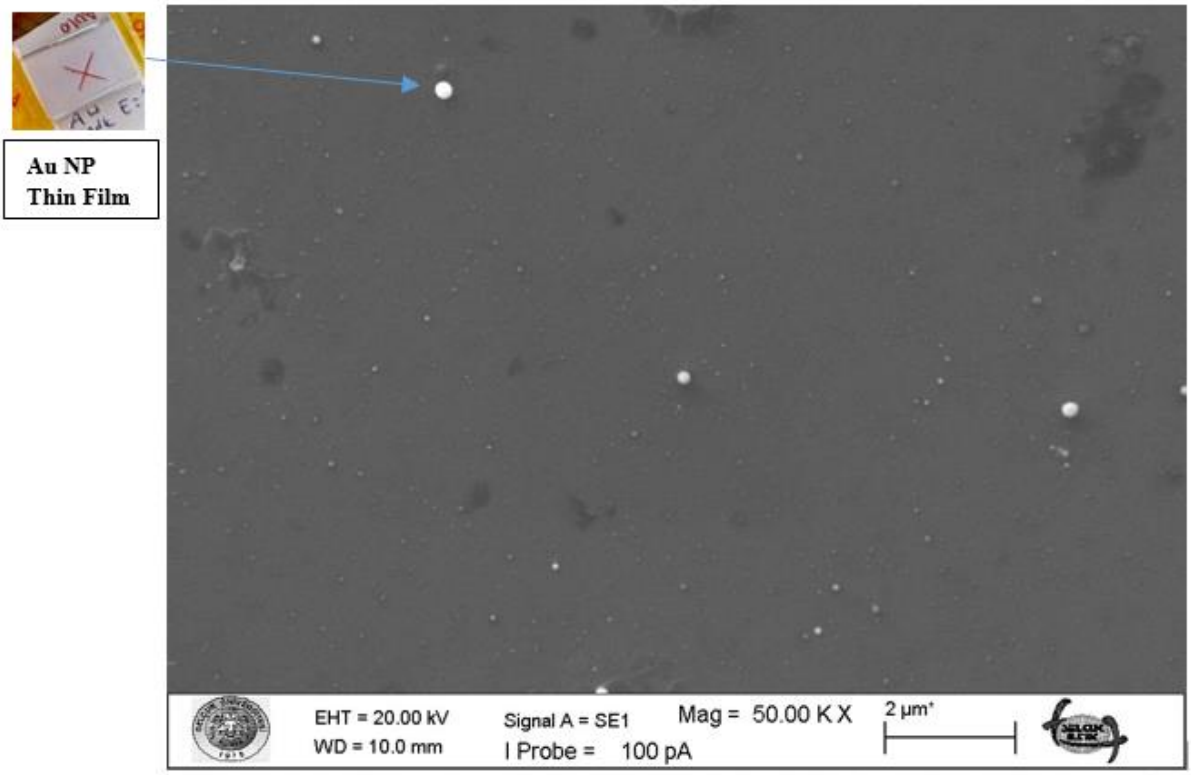

Figure 6. SEM image of plasmonic Au(4) NPs.

The EDS (Energy Dispersive X-ray Spectroscopy) spectrum provided shows the elemental composition of a thin film of Au nanoparticles deposited on a soda-lime glass substrate via Pulsed Laser Deposition shown in the Figure 7. The analysis of the key features can be mentioned as follows. Elements Identified as: Si (Silicon) has a high-intensity peak, likely from the glass substrate. O (Oxygen) stems from the silica (SiO_2) and other oxides in the soda-lime glass. Na (Sodium) has a smaller peak, common in soda-lime glass as Na_2O (sodium oxide). Ca (Calcium) has clearly visible peaks, which is characteristic of CaO (calcium oxide) in soda-lime glass. Mg (Magnesium) has a minor peak, a trace element often present in glass formulations. Au (Gold) has low-intensity peaks corresponding to the deposited gold nanoparticles.

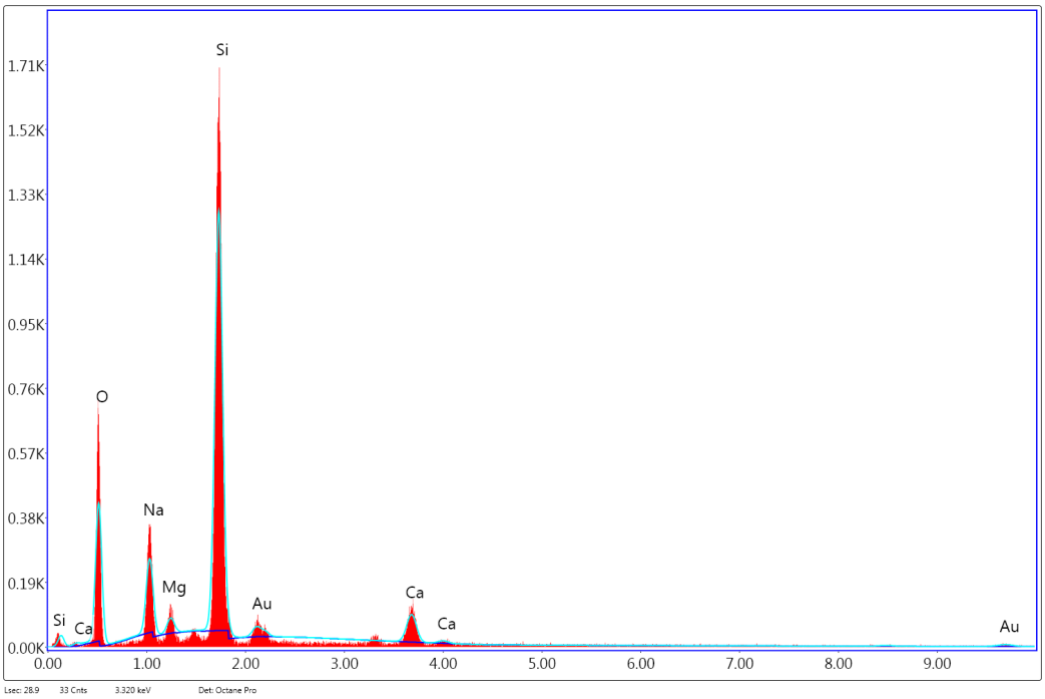

Figure 7. EDS graph of Au(4) NPs produced on soda lime glass by Pulsed laser deposition.

Peak Intensities reveals the following. Si shows the most intense peak, which confirms that the substrate (glass) dominates the composition. O reflects the oxygen bound to silicon (SiO_2) and calcium (CaO). Au peaks for gold (Au) appear at higher energy levels (~2.1 and ~9.7 keV), consistent with characteristic X-rays for Au. However, the intensities are much lower than the substrate peaks, indicating a thin film or low Au concentration. The Au peaks confirm the presence of deposited gold nanoparticles. This result aligns with the expected composition for Au nanoparticles deposited on a soda-lime glass substrate using Pulsed Laser Deposition.

3.4. Photocatalytic Properties of Au NP Thin Film

Industrial dye components, especially those originating from factories, cause environmental pollution and cause significant damage to the environment and human health. The transformation of these organic dye components into clean forms and their reusability in nature is important for the continuity of nature and human life. One of the application areas used to eliminate or reduce environmental pollution caused by wastewater is photocatalysis method. In this study, Metilen Blue (MB) dye, an organic pollutant, was removed by Au NP thin film produced by PLD. First, Au NP thin film was placed into MB organic dye and then a base solution with pH = 10 was added into it. In the dark for 30 min., MB dye was degraded to a negligible scale in the presence of Au NP thin film. However, at the end of 210 min, MB dye was degraded considerably in the presence of Au NP thin film

and a photocatalyst efficiency was determined to be 95.00 % as seen in Fig 8a. Under the condition of no Au NP thin film, the degradation of MB is very low and insignificant.

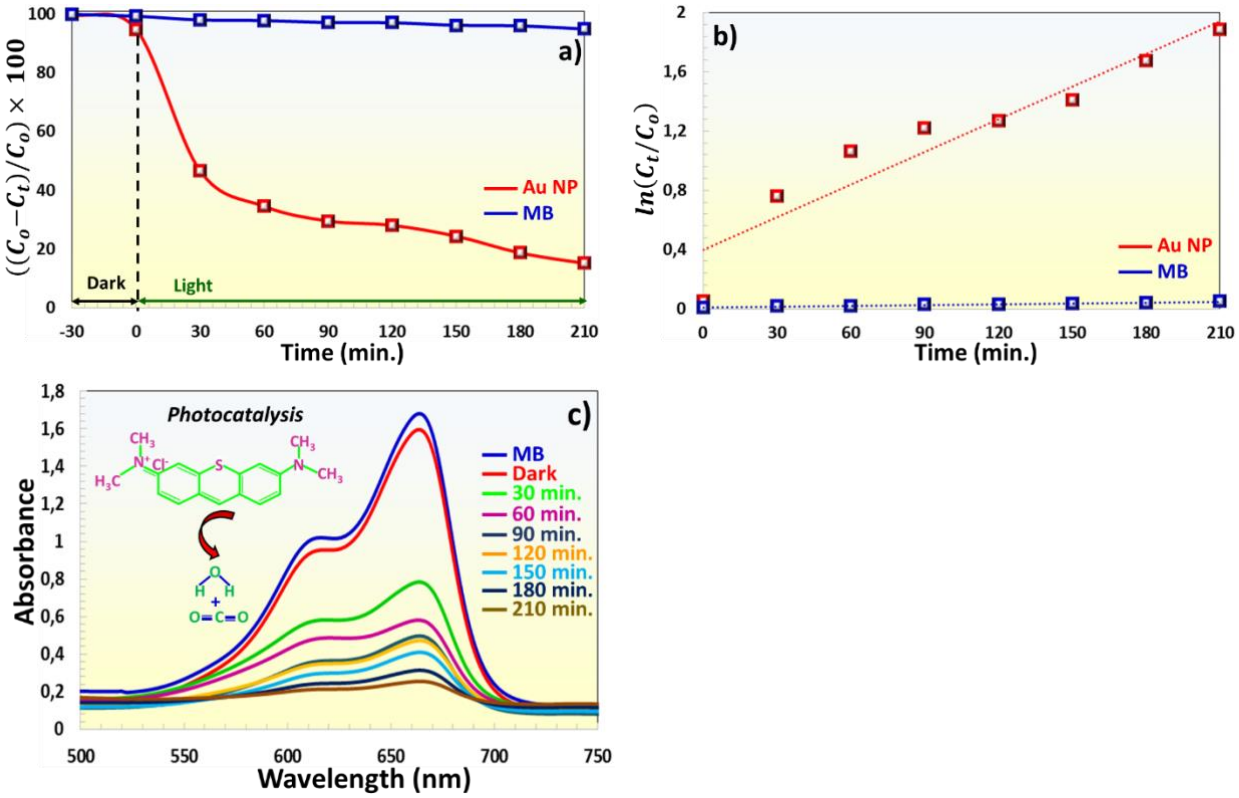

Figure 8. a) The effect on degradation of Au(4) NP thin film grown by the PLD method**, b)** First-order kinetic data of Au NP thin film photocatalyst, and **c)** Real-time absorption spectrum of MB dye in the presence of Au NP thin film (MB degradation mechanism is given as inset in c)

The Langmuir–Hinshelwood first-order kinetic model $\left(ln\left(\frac{C_t}{C_o}\right) = kt\right)$ was used to evaluate the photocatalytic activity of Au NP thin film in Figure 8b [24]. The degradation reaction rate constant of MB dye without using any catalyst was found to be 0.098 min^{-1}. When Au NP thin film photocatalyst was used, the reaction rate constant was determined as 0.39 min^{-1}. The real degradation graph in the Figure. 8c shows the absorption spectrum of Au NP photocatalyst at 210 min. The absorption peak of MB dye is on 666 nm wavelength, when it is exposed to visible light, the intensity of the absorption peak of this dye decreases in the presence of Au NP thin film every 30 min and becomes invisible at the end of 210 min. The reaction mechanism of the photocatalyst is given in the inset image in Figure 8.

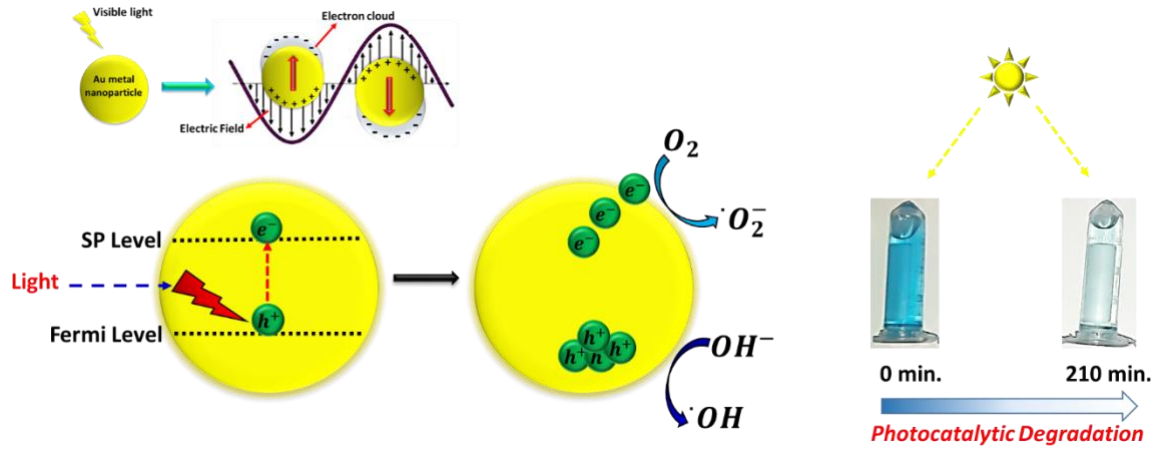

Figure 9. The schematic diagram of MB dye removal by Au NP thin film photocatalysts under visible light

The high-performance photocatalyst event was realized due to LSPR peak property of Au NPs. When visible wavelength light falls on the plasmonic metal Au NP, the electrons in the fermi level of Au are excited and transition to the Surface Plasmon (SP) band [25], causing the formation of $e^- - h^+$ pairs as seen in Figure 9. The released electrons oscillate in resonance as shown in the inset of Figure 9. under the influence of the electromagnetic wave. While the electrons collect on one side of the particle, the holes collect on the other side [26, 27]. The electrons in SP band react with O_2 to form $\cdot O_2^-$ radical [10, 20, 28], while the holes react with water molecules to form hydroxyl ($\cdot OH$) radicals [24]. As a result, the degradation of MB dye occurs and the blue colour of MB dye in Figure 9 became transparent within 210 minutes.

4. Conclusion

This study demonstrates the successful synthesis of Plasmonic AuNPs using PLD and provides a comprehensive analysis of their optical, morphological, structural, and photocatalytic properties. PLD technique proves to be a robust and versatile method for producing high-quality Au NPs, with the ability to precisely control particle size, distribution, and surface characteristics through adjustable deposition parameters. These controllable attributes enable fine-tuning of the NPs' LSPR properties, which are critical for their performance in optical and photocatalytic applications.

Morphological and structural analyses revealed that the synthesized Au NPs possess uniform size distributions, well-defined shapes, and high crystallinity, all of which are essential for stability and functionality. The interplay between particle size and the surrounding medium was shown to significantly influence their LSPR behavior, as characterized by UV-Vis spectroscopy. Structural investigations using X-ray diffraction confirmed that the crystalline nature of the Au NPs, coupled with minimal lattice defects, plays a vital role in enhancing their photocatalytic efficiency.

Photocatalyst performance of Au NP thin film on MB dye degradation was investigated. Au NP thin film photocatalyst efficiency of 95.00% and reaction rate constant 0.39 min^{-1} were calculated. At the end of 210 min, MB dye was degraded and turned into high transparency due to LSPR property of Au NP. The photocatalytic activity of these Au NPs, evaluated through the degradation of organic pollutants under visible light, demonstrated their potential for environmental remediation applications. The strong LSPR effect facilitated efficient light absorption and hot electron generation, which enhanced charge transfer processes and catalytic reaction rates. The results indicate that the photocatalytic performance of Au NPs can be optimized by tailoring their structural and morphological properties during the synthesis process.

In conclusion, PLD emerges as a powerful and clean fabrication method for designing plasmonic Au NPs with highly desirable optical and catalytic properties. The findings of this study provide valuable insights into the relationships between synthesis parameters, NP properties, and their functional performance. These insights contribute to the broader understanding and application of plasmonic materials in fields such as photocatalysis, sensing, and energy conversion. Future work should focus on further optimizing PLD process and exploring hybrid systems where Au NPs can be integrated with other materials to enhance synergistic effects for advanced applications in environmental and energy technologies.

Ethical Statements

The author declares that this document does not require ethics committee approval or special permission. Our study does not cause any harm to the environment.

Acknowledgment

The authors kindly would like to thank Selcuk University, Scientific Research Projects (BAP) Coordination Office for the support with the number 21406007 project. Dicle University, Scientific Research Projects (BAP) Coordination Office for the support.

Conflict of interest

The authors declare no conflict of interest.

Authors Contributions

SYG and IC carried out calculations and wrote the first draft of the manuscript. IC and SYG carried out the experiments. HBG and HSK supervised the projects. All authors discussed the results and contributed to the final manuscript.

References

[1] Ghobashy, M. M., et al., "NPAu NPsin microelectronics advancements and biomedical applications". *Materials Science and Engineering: B*, 301, 117191, 2024.

[2] Zare, I., et al., "Gold nanostructures: synthesis, properties, and neurological applications", *Chemical society reviews*, 51(7), 2601-2680, 2022.

[3] Ramacha ndran, T., et al., "Gold on the horizon: unveiling the chemistry, applications and future prospects of 2D monolayers of NPAu NPs(Au-NPs)", *Nanoscale Advances*, 6(22), 5478-5510, 2024.

[4] Burlec, A.F., et al., "Current overview of metal NPs' synthesis, characterization, and biomedical applications, with a focus on silver and gold NPs''. *Pharmaceuticals*, 16(10), 1410, 2023.

[5] Candan, I., et al., "Sensor properties of plasmonic silver and NPAu NPsproduced by pulsed laser deposition", *Journal of Optoelectronics and Advanced Materials*, 26(5-6), 186-198, 2024.

[6] Agrawal, A., et al., "Localized surface plasmon resonance in semiconductor nanocrystals''. *Chemical reviews*, 118(6), 3121-3207, 2018.

[7] Prabowo, B.A., Purwidyantri, A., Liu, K. C., "Surface plasmon resonance optical sensor: A review on light source technology", *Biosensors*, 8(3), 80 2018.

[8] Candan, İ., et al., "Biosensor Properties Of Plasmonic Silver Nps Produced By Pld", *Middle East Journal of Science*, 7(2), 112-122, 2021.

[9] Ahmad, I., et al., "A comprehensive review on the advancement of transition metals incorporated on functional magnetic nanocomposites for the catalytic reduction and photocatalytic degradation of organic pollutants". *Coordination Chemistry Reviews*, 514: 215904, 2024.

[10] Dhiman, M., "Plasmonic nanocatalysis for solar energy harvesting and sustainable chemistry", *Journal of Materials Chemistry A*, 8(20), 10074-10095, 2020.

[11] Gellé, A., Moores, A., "Plasmonic NPs: Photocatalysts with a bright future", *Current Opinion in Green and Sustainable Chemistry*, 15, 60-66, 2019.

[12] Kukreja, L.M., et al., "Pulsed laser deposition of plasmonic-metal nanostructures", *Journal of Physics D: Applied Physics*, 47(3), 034015, 2013.

[13] Gezgin, S.Y., Kepceoğlu, A., Kılıç, H.Ş., "An investigation of localised surface plasmon resonance (LSPR) of Ag NPs produced by pulsed laser deposition (PLD) technique", AIP Conference Proceedings, AIP Publishing LLC, 2017.

[14] Gezgin, S.Y., Kepceoğlu, A., Kılıç, H.Ş., "An experimental investigation of localised surface plasmon resonance (LSPR) for Cu NPs depending as a function of laser pulse number in Pulsed Laser Deposition", AIP Conference Proceedings, AIP Publishing LLC, 2017.

[15] Yu, J., et al., "Recent Advances on Pulsed Laser Deposition of Large-Scale Thin Films", *Small Methods*, 8(7), 2301282, 2024.

[16] Dal'Toé, A.T., et al., "Lanthanum doped titania decorated with silver plasmonic NPs with enhanced photocatalytic activity under UV-visible light", *Applied Surface Science*, 441, 1057-1071, 2018.

[17] Ou, W., et al., "Plasmonic metal nanostructures: concepts, challenges and opportunities in photo-mediated chemical transformations", *Iscience*, 24(2), 101982, 2021.

[18] Desseigne, M., et al., "Plasmonic Photocatalysts Based on Au NPs and WO3 for Visible Light-Induced Photocatalytic Activity". *Catalysts*, 13(10), 1333, 2023.

[19] Yuan, L., et al., "Sustainable chemistry with plasmonic photocatalysts", *Nanophotonics*, 12(14): 2745-2762, 2023.

[20] Khan, M.E., Cho, M.H., Surface plasmon-based nanomaterials as photocatalyst, Advanced Nanostructured Materials for Environmental Remediation, 25, pp. 173-187, 2019.

[21] Sundararajan, B., Kumari, B.R., "Novel synthesis of NPAu NPsusing Artemisia vulgaris L. leaf extract and their efficacy of larvicidal activity against dengue fever vector Aedes aegypti L", *Journal of Trace Elements in Medicine and Biology*, 43, 187-196, 2017.

[22] Oliveira, A.E.F., et al., "Gold NPs: a didactic step-by-step of the synthesis using the turkevich method, mechanisms, and characterizations", *Analytica*, 4(2), 250-263, 2023.

[23] Balasubramani, G., et al., "GC–MS analysis of bioactive components and synthesis of gold NP using Chloroxylon swietenia DC leaf extract and its larvicidal activity", *Journal of Photochemistry and Photobiology B: Biology*, 148, 1-8, 2015.

[24] Dursun, S., et al., "Investigation of photocatalytic activity (under visible light) of ultrathin CZTS films produced in different thicknesses by PLD method", *Optical and Quantum Electronics*, 55(2), 166, 2023.

[25] Yiğit Gezgin, S., Kiliç, H. Ş., "The effect of Ag plasmonic NPs on the efficiency of CZTS solar cell: an experimental investigation and numerical modelling", *Indian Journal of Physics*, 97(3), 779-796, 2023.

[26] Gezgin, S.Y., Kepceoğlu, A., Kılıç, H. Ş., "An investigation of localised surface plasmon resonance (LSPR) of Ag NPs produced by pulsed laser deposition (PLD) technique", AIP Conference Proceedings, AIP Publishing, 2017.

[27] Gezgin, S.Y., Kepceoğlu, A., Kılıç, H. Ş., "An experimental investigation of localised surface plasmon resonance (LSPR) for Cu NPs depending as a function of laser pulse number in Pulsed Laser Deposition", AIP Conference Proceedings, AIP Publishing, 2017.

[28] Verma, P., et al., "Plasmonic nanocatalysts for visible-NIR light induced hydrogen generation from storage materials", *Mater. Adv.* 2, 880–906, 2021.